Arterial path selection to measure pulse wave velocity as a surrogate marker of blood pressure

2017 Biomed. Phys. Eng. Express 3 015022

(http://iopscience.iop.org/2057-1976/3/1/015022)

Biomedical Physics & Engineering Express

PAPER

RECEIVED
7 December 2016

REVISED
20 January 2017

ACCEPTED FOR PUBLICATION
23 January 2017

PUBLISHED
8 February 2017

Arterial path selection to measure pulse wave velocity as a surrogate marker of blood pressure

M Radha[1,2], G Zhang[1,2], J Gelissen[1], K de Groot[1], R Haakma[1] and R M Aarts[1,2]

[1] Personal Health, Philips Research, Royal Philips High Tech Campus 34, 5656 AE, Eindhoven, The Netherlands
[2] Electrical Engineering, Eindhoven University of Technology Flux, floor 7, PO Box 513, 5600 MB, Eindhoven, The Netherlands

E-mail: mustafa.radha@philips.com

Keywords: photoplethysmography, pulse arrival time, systolic blood pressure, sensor locations, hemodynamics, pulse wave velocity, pulse propagation

Abstract

The velocity of the propagating arterial pulse wave (pulse wave velocity, PWV) has been proposed as an unobtrusive and possibly continuous surrogate measure of systolic blood pressure (SBP). PWV is derived from the arrival time of the blood pulse at a peripheral arterial location, most often the finger. Reported performances were not yet accurate enough for clinical application but good enough as an unobtrusive surrogate in other settings. However, the finger PPG is not an ideal location in the home setting as it obstructs hand movement and can suffer from peripheral vasomotion and orthostatic pressure changes. In this paper we examine the viability of other pulse arrival locations for the measurement of PWV. PWV was derived to the finger (most common location), wrist (less obtrusive location), ear (more proximal) and ankle (more distal). Correlation analysis for PWV from each location with SBP was performed and the calibration procedure was studied. Wrist PWV accuracy is found to be comparable to finger PWV in terms of correlation and estimation error with SBP. The ear PWV, being a theoretically favorable location, is shown to have a larger inter-subject variance in the calibration procedure compared to other locations. Ankle PWV shows stable calibration parameters across subjects but Bland-Altmann analysis reveals unusual error trends. In conclusion, while results indicate that all sensor locations are usable to some extent, there are still some distinct properties associated with each sensor location that should be taken into account when designing an SBP algorithm based on PWV.

1. Introduction

Blood pressure (BP) is one of the major vital signs and a strong indicator of cardiovascular health. The prevalence of pathologically high BP (i.e. hypertension) is higher than ever (Cutler *et al* 2008) and new studies reveal that even moderate elevations in blood pressure that were not considered pathological in the past are also linked to cardiovascular events (SPRINT Research Group 2015). These trends are met with an increasing demand for better blood pressure management, of which an essential ingredient is the measurement of BP. Next to the clinical use of BP measurement for hypertension diagnosis and other haemodynamic complications (Chase *et al* 2004, Greenland *et al* 2010), home blood pressure monitoring is also important (ESH/ESC 2013). Currently, individuals are capable of self-monitoring BP at home by using a standard oscillometric pressure cuff. This type of devices calculate the systolic and diastolic blood pressure (SBP and DBP) which correspond respectively to the peak pressure in the artery as the pulse wave is passing through and the lowest pressure in-between beats, two of the most recognized BP parameters. However, these pressure cuffs lack portability and their inflation is obtrusive and painful. These factors make the measurement of BP a burden on the individual, decreasing the tendency of users to routinely self-monitor BP and thus negatively contribute to blood pressure management. This motivates research into new methods of surrogate BP measurement. Besides the cuff, a few solutions have been proposed over the past decades (Pickering *et al* 2005). However, these products were not designed with home

measurement in mind: while they enable long-term continuous measurement, they are still bulky and obtrusive (e.g. vascular unloading technique) or difficult to operate (e.g. applanation tonometry). For an overview of current BP measurement methods, the reader is referred to (Pickering *et al* 2005).

1.1. Pulse wave velocity

One of the most promising surrogate methods for BP measurement is pulse arrival time (PAT), which is the time the pulse wave takes to arrive at an arterial site after ejection from the heart. PAT is an indicator of pulse wave velocity (PWV), which can be derived by dividing the length L of the traversed arterial segment over PAT:

$$\mathrm{PWV} = \frac{L}{\mathrm{PAT}}. \tag{1}$$

The onset of ventricular ejection is most often measured with electrocardiogram (ECG) even though it is known that there is a slight time difference between the ECG's R-peak and the actual start of pulse transit, known as the pre-ejection period (Payne *et al* 2006, Zhang *et al* 2011). Other more accurate pulse onset measurement methods exist but are either more difficult to operate (e.g. phonocardiogram), noise-prone (e.g. seismocardiogram and ballistocardiogram Inan *et al* 2015) or expensive (e.g. ultrasound). Pulse arrival is conveniently measured with photoplethysmography (PPG), an easy to use and affordable sensor. PPG works by illuminating the skin with light and capturing the intensity of the reflected light from the skin. The intensity of reflection depends on how much of the light is absorbed by the skin. By choosing a light frequency that is absorbed by blood, it is possible to measure the pulsatile blood flow. Multiple morphological markers on the PPG pulse can be used for the detection of pulse arrival (Kortekaas *et al* 2012). An important mediator in the reflection profile is the contact pressure of the PPG sensor: a loose contact pressure could allow ambient light to be picked up by the photodetector while a high pressure can decrease blood perfusion locally, both reducing the quality of the signal (Teng and Zhang 2007).

1.2. The PWV-BP relation

PWV is classically related to BP through the Moens-Korteweg equations (Proença *et al* 2010). The relationship between BP and PWV can be derived from this equation as follows:

$$\mathrm{PWV} = \sqrt{\frac{E_0 e^{\gamma \mathrm{BP}} \cdot h}{2\rho \cdot r}}, \tag{2}$$

where E_0 is the elastic modulus at zero pressure, ρ is the blood density, h is the vessel radius, r is the vessel wall thickness and γ is a coefficient depending on the particular vessel. This function can be rewritten as:

$$\ln(\mathrm{PWV}^2) = \frac{\ln(E_0 h)}{2\rho r} + \gamma \mathrm{BP} \tag{3}$$

which can be simplified as:

$$\mathrm{BP} = \frac{2}{\gamma}\ln(\mathrm{PWV}) - \frac{\ln(E_0 h)}{2\rho r \gamma}. \tag{4}$$

Thus, when assuming that h, r, γ and and ρ stay more or less constant from measurement to measurement (in comparison with PWV), it can be proposed that there is a linear dependence between BP and ln(PWV) (Peter *et al* 2014, Mukkamala *et al* 2015). Thus, a calibration for each arterial segment (and each person) looks as follows: $\mathrm{BP} = a \cdot \ln(\mathrm{PWV}) + b$, where $a = \frac{2}{\gamma}$ and $b = -\frac{\ln(E_0 h)}{2\rho r \gamma}$. While many encouraging results have been achieved with this way of working, it has also been evident that the approach has its limitations. For clinical use, this theoretical model did not prove to be accurate enough to deal with the complex and abnormal physiologies of patients (Smith *et al* 1999) and it has been found to be an inaccurate marker for both diastolic and mean arterial pressure (Payne *et al* 2006). However, for SBP many positive results have been obtained in various contexts (Solà *et al* 2009, Gesche *et al* 2012, Tang *et al* 2016).

Recently, wearable technology for health monitoring has enjoyed a wide use and is becoming part of everyday life. This has enabled sophisticated health monitoring methods to become accessible to many. Such technology that is not primarily intended to diagnose or treat disease falls under the category of *general wellness* technology. These devices do not have to meet the rigorous standards of medical equipment while still can play a supplementary role in maintaining a healthy lifestyle (U.S. Food and Drug Administration 2015). PWV as a surrogate SBP measurement method could be positioned within this landscape. However, there are still practical issues that need to be resolved before PWV-based SBP measurement can be embodied within an application that is readily deployable. While the theoretical model from equation (4) holds in controlled conditions, in a real embodiment there are a number of practical issues that can heavily impact accuracy.

1.3. Practical issues

The most common pulse arrival location in literature used to study PWV as a surrogate marker of SBP is on the finger (Wong *et al* 2009, Peter *et al* 2014, Mukkamala *et al* 2015, Sun *et al* 2016b), mainly because of the historical reason that the finger PPG clip has been an integral part of clinical practice (used for the assessment of blood oxygen saturation), making them more accessible for clinical studies (Yoon *et al* 2002, Wijshoff *et al* 2016). While this has enabled fundamental research on the topic, it is not the most ideally suited location for wearable technology as it hampers manual work with the hands. An obvious alternative could be to measure at the wrist in a watch-type device, a

relatively unobtrusive location which is already in use for the measurement of other health markers (Rupp and Balkin 2011, Valenti and Westerterp 2013, van Andel *et al* 2015).

Yet, the measurement of PWV to the lower arm suffers from physiological factors that can influence the BP relationship. In the simplified model presented in equation (4) it is assumed that the arterial properties γ, r, E_0 and h are constant. This assumption does not hold by default as the pulse propagates through a series of vessels with changing properties. This non-uniformity in the vessel path increases as the pulse arrival location is more distal.

Another effect is that the vessel radius h and the wall thickness r can be altered within peripheral arteries by muscle tissue in the arterial wall called smooth muscles (Mukkamala *et al* 2015). Smooth muscles are activated by the autonomic nervous system to control blood flow. This is done in response to stressors such as physical exercise or for thermoregulatory purposes.

Another limitation of the Moens-Korteweg equation is that it assumes the vessel through which the pulse propagates to be fixed in altitude with respect to the heart. This only holds in very specific conditions. When the human is not limited in mobility, posture changes can have significant impact on the relationship between PWV and BP. Attempts have been made to extend the Moens-Korteweg model to account for this (Poon *et al* 2006, McCombie 2008, Thomas *et al* 2015) but ideally posture change should be avoided to ensure a reliable measurement.

Thus, ideally, the vessel over which PWV is derived should be (1) as fixed in altitude as possible relative to the heart, (2) contain a minimum of smooth muscle tissue and (3) be as uniform as possible. Requirements two and three can be controlled by selecting a location that is relatively proximal to the heart, ensuring a short traversal path and little smooth muscles. The first requirement can be met by choosing a pulse arrival site on a limb that does not change in altitude relative to the heart. This invites for the measurement of PWV to the head (He *et al* 2012) or to the chest (Solà *et al* 2009).

While measurement of PWV to a proximal location seems to alleviate many of the practical issues, it also has its drawback. In practice, SBP is always measured at the brachial artery with a cuff wrapped around the upper arm. As this is a relatively peripheral location the measured BP is also indicative of peripheral BP. When measuring PWV centrally, the obtained BP predictions could therefore also be indicative of central BP and thus may reflect central rather than peripheral hemodynamics. In clinical practice this is already an accepted parameter, in which case PWV is derived from the time difference between the femoral and carotid pulse wave arrival (femoral-carotid PWV). This is in contrast to the PWV that is defined in this paper, which is sometimes differentiated from femoral-carotid PWV as R-wave gated PWV (Naschitz *et al* 2004). There are known differences between central and peripheral BP, however it has also been shown that the two parameters can be predicted from each other to a certain extent (Karamanoglu *et al* 1993).

A final issue is the accuracy of the PWV measurement itself. When PWV is measured over a short arterial segment, small measurement errors in PAT can propagate into large estimation errors of SBP. Thus, it could be that the use of very long arterial segments would provide a more accurate measurement of PWV and thus reduce the sources of error. This could be achieved by measuring PWV over very long arterial segments, with pulse arrival locations at the extremities of the body such as on the ankle. The ankle as a pulse arrival location has been studied in the past for hemodynamic measurement (Nitzan *et al* 2002, Foo *et al* 2007, Ankle Brachial Index Collaboration 2008, Padilla *et al* 2009). It could be used to derive the Ankle-Brachial Index (revealing peripheral artery disease) or the measurement of PWV in children (where other sensor locations might become inaccessible due to small limbs).

In summary, there are practical issues related to each arterial site on which pulse arrival can be measured. More proximal locations such as the head satisfy the conditions of the Moens-Korteweg equations better but could potentially be insensitive to peripheral blood pressure variations, while very distal locations could reduce estimation error in pulse arrival but may be confounded by a variety of factors. The use of the lower arm could be a middle-way between both locations, but there has been no exploration whether the non-ergonomic finger clip can be replaced by a wrist-worn device.

2. Research goals

The goal of this study is to show how the choice of arterial site affects the obtained PWV and its relation to SBP. Specifically, the goal is to find out how PWV to proximal and very distal arterial sites perform in predicting SBP, relative to PWV measured to the finger (as the default location). The secondary goal is to confirm that PWV measured to the finger is equivalent to PWV measured to the wrist. These tests help to understand whether it is feasible to measure PWV as a surrogate marker of BP in a more practical way than using a PPG clip on the finger.

3. Materials

Twenty volunteers participated in the current trial. Three participants were excluded from the data analysis due to untrustworthy signals from the reference device (CNAP blood pressure monitor 500, CNSystems), showing a high jump in blood pressure before and after recalibration. The remaining 17 participants (mean age 31.4 years; 8 female) were

Table 1. Participant characteristics.

Subject	Age (years)	Sex	Weight (kg)	Height (cm)
S1	42	Male	85	178
S3	27	Male	83	183
S4	24	Female	62	164
S5	24	Female	68	172
S6	53	Male	83	180
S7	25	Male	82.5	182
S8	32	Female	66	168
S9	28	Male	78	185
S10	22	Female	53	168
S11	22	Female	53	168
S12	58	Male	81.5	182
S13	27	Male	75	182
S16	27	Female	65	175
S17	31	Female	59	167
S18	35	Male	101	199
S19	28	Male	75	175
S20	28	Male	74	180
Average	31	41% F	73	177

recruited within Philips Research. More detailed subject characteristics are shown in table 1. Prior to the start of the trial, participants received an oral and written explanation of the study procedure. All participants provided written consent. The observational protocol was approved by the internal ethics committee for Biomedical Experiments of Philips Research Eindhoven in conformity with the declaration of Helsinki. Exclusion criteria included: suffering from any chronic disease (such as diabetes, cardiovascular and pulmonary diseases), functional and cognitive impairments, use of medication affecting the hormonal, metabolic or cardiovascular system, pregnancy and incapability to perform sport related exercises.

Subjects were seated in a normal chair behind a cycle ergometer, positioned so that the full extension of the knee was not reached during a complete cycle motion. Their left arm was resting on a table, ensuring stability and arm muscle relaxation. Subjects were outfitted with four PPG sensors; one on the right earlobe (TSD200, Biopac), one on the right index finger (TSD200, Biopac), one on the dorsal side of the right wrist, proximal of the ulnar styloid process (Philips WeST, similar to the device validated in Valenti and Westerterp 2013) and an identical device on the distal side of the right ankle, proximal of the fibula styloid process. The Biopac sensors are attached with a spring-based clip, ensuring approximately the same contact force regardless of the size of the finger and ear. The Philips WeST devices were held in position with sweatbands. The experimenter ensured that the sweatbands were tight enough to keep the PPG sensors in place without being too tight for the participant. Blood pressure was recorded using a CNAP blood pressure monitor 500 (CNSystems), placing the cuff around the left upper arm and the finger cuffs on the index and middle finger of the left hand. All sensors were connected to a Biopac acquisition system (Biopac) sampling at 1000 Hz ensuring synchronized recordings of the signals. A schematic overview of the measurement setup is given in figure 1.

Participants were instructed to ensure a comfortable position, keeping the right foot during the rest periods at the lowest point and returning to this point after each cycling session. The protocol was similar to the one used in (Sun *et al* 2016a), starting with five minutes of rest followed by three sessions, each consisting of five minutes cycling and five minutes rest.

4. Methods

4.1. Signal processing

The raw PPG signals were filtered. Baseline PPG modulation due to respiration was removed with a high-pass Butterworth filter (cut-off = 0.4 Hz). Subsequently, a low-pass filter was applied to remove high-frequency noise (cut-off = 10 Hz).

After data cleaning, the quality of each heart beat on each PPG sensor was examined with a template-matching algorithm (Li and Clifford 2012). As the experiment involves cycling, the ankle typically had a higher rejection rate due to motion artifacts. The ear, being always at the same hight above the heart during the experiment, typically had the lowest rejection rate. As a compromise between quantity and quality, a rejection threshold of 0.7 was used, which corresponds roughly to the rejection of the most intensive cycling periods. However, the gradual decrease of blood pressure just after exercise bouts is not rejected, which ensures a sufficient level of variation in BP for correlation analysis.

ECG R-peaks were localized with an enhanced variation of the Hamilton-Thompkins QRS detector (Fonseca *et al* 2014).

For the detection of the pulse arrival, three possible methods could be used (Rapalis *et al* 2014). These are (1) the foot of the PPG pulse, (2) its maximal rising slope or (3) the systolic peak. These are illustrated in figure 2. All three methods were used and one was selected empirically based on correlation (see section 4.2 and 5) for results. It is important to use the same pulse arrival detector on all PPG signals as the selected method will affect measured PAT.

Using the computed PAT measurements, PWV was determined, for which the PAT was adjusted for the arterial segment length. The segment length per sensor location can be estimated from the subject height using the known standard proportions of the human body, taken from (Winter 2009). This has been done before for the estimation of PWV to the wrist in (Gesche *et al* 2012). A body correlation factor (BDC) is derived which expresses the length of an arterial pathway relative to total body height: $PWV = (BDC * h)/PAT$. Here, h is the person's

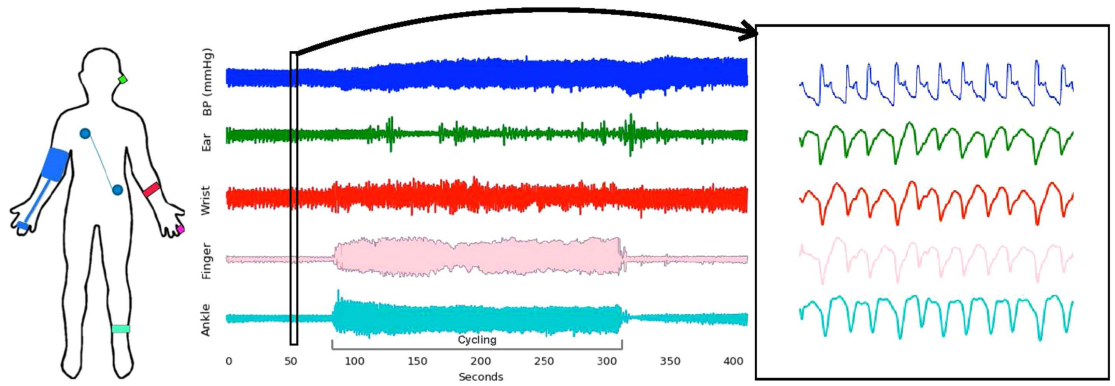

Figure 1. Schematic overview of the measurement set-up and acquired signals. The signal of lead-II ECG (ground lead not shown) was omitted.

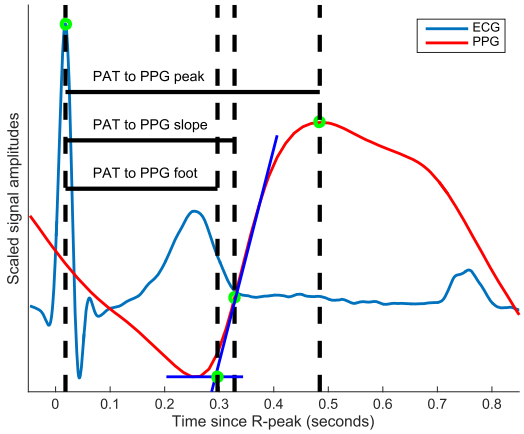

Figure 2. Landmarks and time intervals visualized for a cardiac cycle. ECG is in blue and wrist PPG is in red. The red crosses denote (from left to right) the ECG R peak, the PPG onset, maximum slope and peak. The horizontal black lines denote the three pulse arrival time intervals.

height in meters (m) and PAT is in seconds (s), resulting in PWV in m s^{-1}. The BDC was 0.50 for the wrist, 0.52 for the finger, 0.18 for the ear and 0.80 for the ankle. These population averages do not take into account the *ape factor*, which is an individual variation in arm and leg length from the general average. However this is not a limitation for the trend analyses in this study.

Finally, the continuous blood pressure measurement from the CNAP is used to determine SBP values for each considered beat. For this, a single beat was isolated between two consecutive R peaks on the ECG and the maximum value was taken as the SBP.

4.2. Statistical analysis

First off, the different PPG markers for pulse arrival (see figure 2) are compared in terms of correlation with SBP. The selected signal processing method is then used to further study both the distribution of PWV and its relation to blood pressure from one sensor location to another.

Once the signal processing method is selected, the calibration procedure will be studied from subject to subject. It was explained in the introduction that a mapping between SBP and PWV is possible of the form $SBP = a * \ln(PWV) + b$. The parameter a is proportional to the artery-specific property γ, namely $a = \frac{2}{\gamma}$ (see equation (4)). It intuitively corresponds to the responsiveness of BP to SBP as its unit is $mmHg/\ln(\frac{m}{s})$. Thus, the parameter a will be examined between different sensor locations. The focus is on understanding which of the sensor locations have a more stable a across subjects. Such a location could potentially suffer less from calibration problems.

Finally, using the calibrated regression functions, the PWV will be used to predict SBP for all subjects. The results are visualized per sensor location and statistics are given about the accuracy of each location, in terms of the correlation as well as the mean absolute error between predicted SBP and true SBP.

5. Results and discussion

5.1. PPG markers of pulse arrival

The different PPG markers of pulse arrival were tested in terms of the number of beats for which the PPG marker was successfully detected. Subsequently the correlation was computed per subject between SBP and the the PWV derived with that particular PPG marker. In table 2 an overview is given of this analysis in terms of averages and standard deviation over the subjects. In figure 3 boxplots are presented of the obtained correlations.

For all sensor locations the onset of the pulse was detected in more beats than any other marker of pulse arrival. The slope method resulted in the highest correlation with SBP for wrist, finger and ankle, while on the ear the onset method showed a slightly better correlation with SBP. The peak-based PPG marker performed worst on all arterial sites: the peak was the most difficult to detect leading to the smallest number of found beats and its correlation with SBP was lowest.

Table 2. Averages and standard deviations, over subjects, per PAT method, for the number of beats analyzed (column 1) and the correlation of systolic blood pressure (column 2) with the PAT method.

	# of beats	Corr SBP
wrist onset	1670 ± 421	−0.61 ± 0.21
wrist slope	1659 ± 429	−0.66 ± 0.18
wrist peak	1649 ± 429	−0.54 ± 0.19
ankle onset	1219 ± 486	−0.42 ± 0.27
ankle slope	1214 ± 486	−0.47 ± 0.27
ankle peak	1172 ± 478	−0.38 ± 0.32
finger onset	1527 ± 429	−0.63 ± 0.20
finger slope	1525 ± 429	−0.65 ± 0.19
finger peak	1519 ± 430	−0.53 ± 0.23
ear onset	1620 ± 295	−0.65 ± 0.16
ear slope	1561 ± 351	−0.60 ± 0.21
ear peak	1552 ± 349	−0.46 ± 0.20

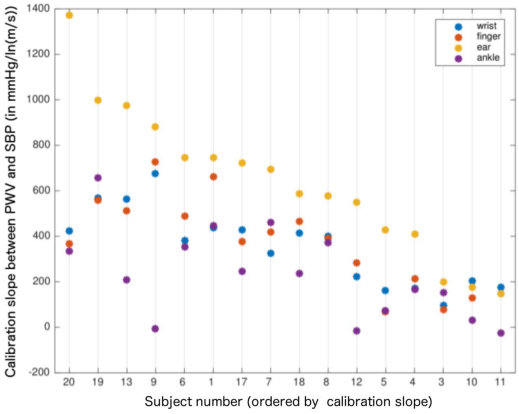

Figure 4. The factor a over subjects per sensor location, where a is a parameter fitted per subject in the function $\text{SBP} = a * \ln(\text{PWV}) + b$.

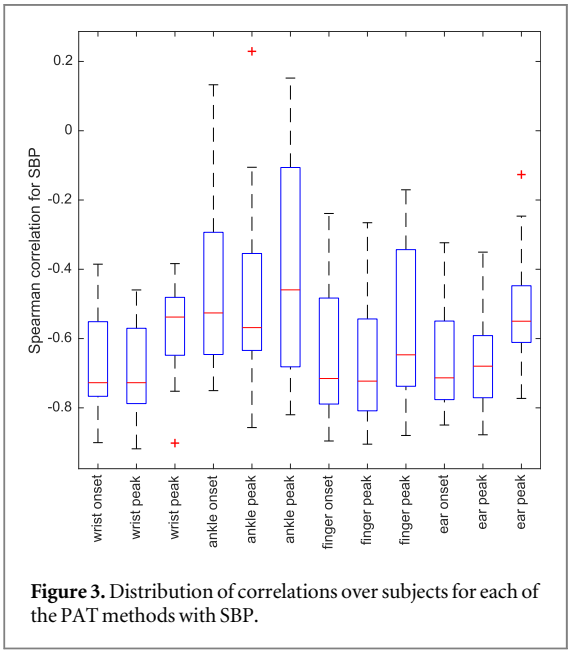

Figure 3. Distribution of correlations over subjects for each of the PAT methods with SBP.

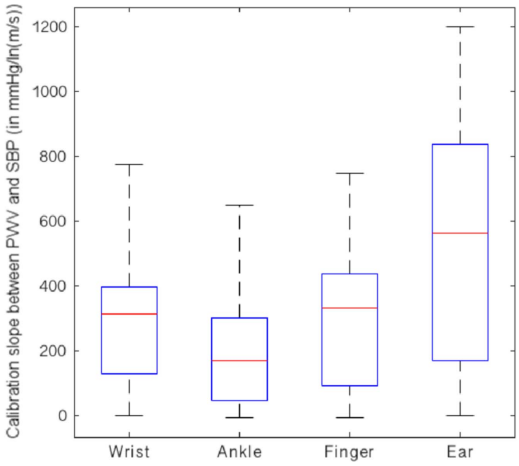

Figure 5. Boxplot per location of the calibration slope a.

Based on this, it was chosen to use the maximal slope of the PPG pulse as an indicator pulse arrival as it performs very well for all sensor locations.

5.2. Site-related differences in PWV and its relation to SBP

The PWV-SBP ratio a was derived per sensor location for all subjects. In figure 4 these calculated values of a are given. In figure 5 the boxplots are shown of values a for all subjects for a certain sensor location.

The differences in a from one sensor location to another were significant (using a paired samples t-test) for ear and wrist ($p < 0.0001$), ear and ankle ($p < 0.0001$), ear and finger ($p < 0.0001$), finger and ankle ($p < 0.0051$) and ankle and wrist ($p < 0.01$). The only exception was the comparison between the wrist and the finger, where no statistical differences were found.

It can also be observed in figure 4 that the parameters a are correlated across subjects: people with a small a in one sensor location also have the tendency to have a small a on another sensor location. Pearson's correlation analysis shows that the wrist is highly correlated with finger ($c = 0.88$) and ear ($c = 0.85$) and moderately correlated with the ankle ($c = 0.55$). The ear and ankle are also correlated ($c = 0.67$) while the ear and finger have a high correlation as well ($c = 0.89$).

However, there are also clear differences between sensor locations. The factor a is the highest for the ear: small changes in ear PWV come with large changes in SBP. Also the inter-subject variance is highest for the ear (see also ear confidence interval in figure 5). On the other end of the spectrum, for subjects with an overall lower PWV, the values of a are very close to each other regardless of the sensor location. For subjects S17, S3, S10 and S16 the differences in a from one sensor location are very small compared to the differences observed within subjects with high PWV such as S19, S9 and S13. These findings hint at the mediating effect of peripheral resistance on BP: at the proximal ear (with relatively little vasomotion in the pathway) there

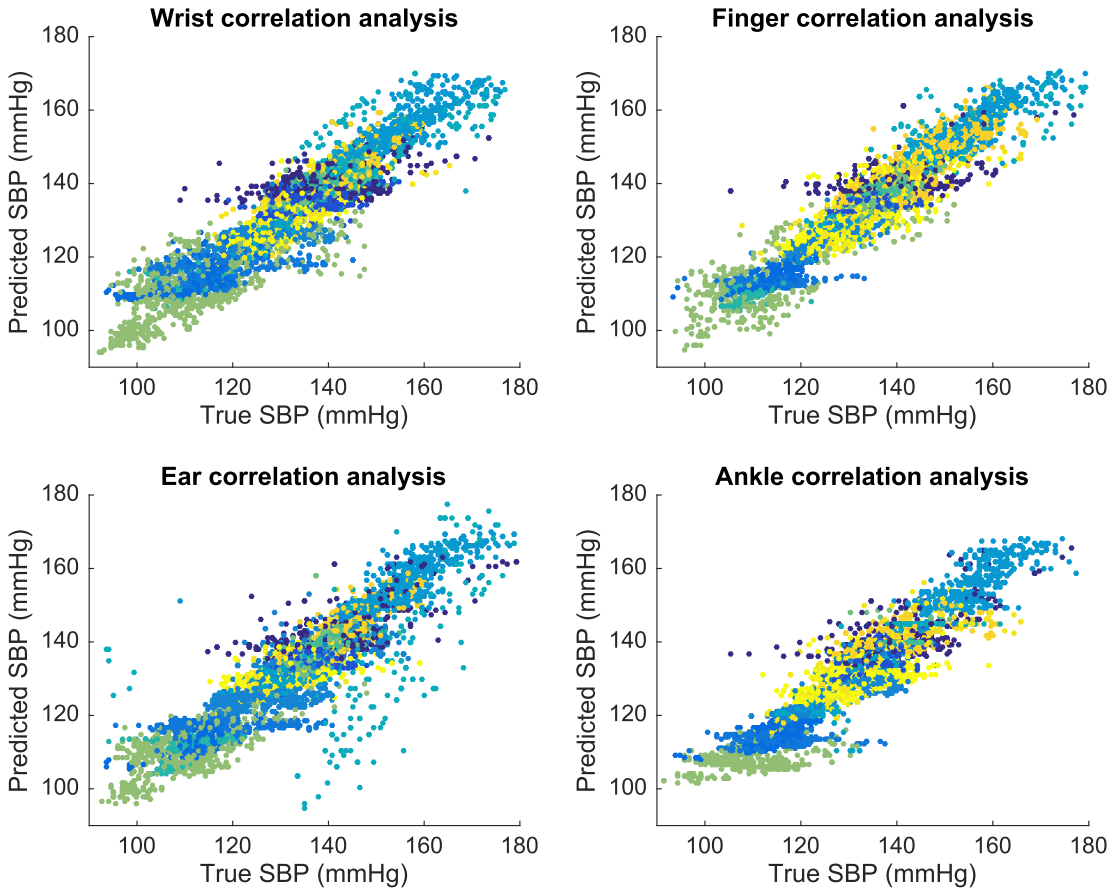

Figure 6. The relation between pulse arrival time to the maximal slope of the PPG and systolic blood pressure (per beat, for each sensor). Each shade denotes a different subject. Pearson's correlation (C) and mean absolute error (MAE) are reported in the titles of the figures. Half of the data points was chosen at random for visualization to increase readability.

is a large inter-subject variance but as the sensor location is placed more distally, it is observed that PWV is normalized to a target level by the periphery, thus reducing inter-subject variance.

5.3. Prediction of SBP with PWV to different arterial sites

In table 2 the correlations between SBP and PWV from all arterial sites is presented, however that correlation was averaged over all subjects, concealing many details. Therefore, the calibration function for each subject was applied to obtain SBP from PWV. The resulting SBP and PWV values are visualized in figure 6. Spearman's correlation was 0.93 for all sensor locations. In figure 7 the Bland-Altmann analyses are given that correspond to the same data. Mean errors for all sensors were 0 mmHg except for ear (mean error of 1 mmHg). The confidence interval (CI) of the error was respectively 11 mmHg, 10 mmHg, 14 mmHg and 11 mmHg for wrist, finger, ear and ankle.

The correlation between SBP and PWV is evident, though it is also observed that the predictions are not an exact match. In all sensor locations, a seemingly white noise is visible in the correlation analyses of figure 3. The Bland–Altmann figures show that this noise has $\mu \approx 0$ mmHg and a 90% CI of 20 to 26 mmHg. This noise could be attributed to the effect of breathing on the relationship between PWV and BP. The continuous rhythmic variations in intra-thoracic pressure due to breathing cause modulations in heart rate and PWV. The variations in PWV have been observed in (Drinnan *et al* 2001) to be maximally 14 ms to the finger. For comparison, in our study the PWV to finger was 2.6 m s^{-1} on average, thus a change of 14 ms would impact PWV with 0.06 m s^{-1}. This would correspond to a 21 mmHg for the average subject, which is close to the 90% CI of the finger of 20 mmHg.

5.3.1. Wrist

The Bland-Altmann analyses for the wrist and finger reveal comparable statistics: both have a small estimation bias of equal magnitude and a high correlation. In section 5.2 it was also shown that the calibration parameters are very similar between wrist and finger. Thus, the evidence suggests that the wrist PPG could replace the finger PPG with little risk. However, it is not known which of the sensor locations is impacted more by thermoregulation induced vasocontriction.

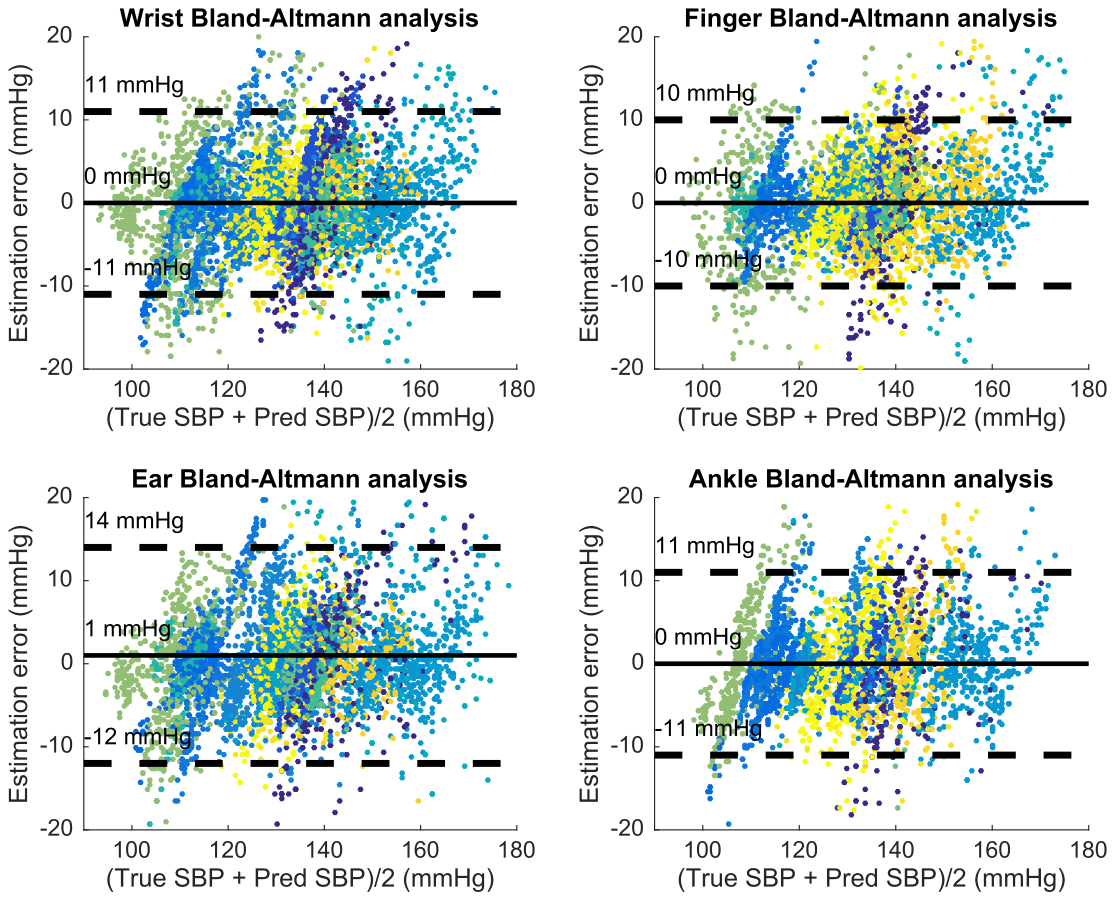

Figure 7. Bland-altmann analysis of the results presented in figure 6. Each shade denotes a different subject. Half of the data points was chosen at random for visualization to increase readability.

5.3.2. Ear

While correlation analysis for the ear PWV yielded a similar result as to wrist and finger, the Bland-Altmann figure reveals a higher error range caused by more outlier points. This could be due to the earlier explained differences between proximal and distal locations for pulse arrival measurement.

5.3.3. Ankle

The PWV to the ankle becomes more noisy with higher PWV levels. This is likely due to the motion artefacts during cycling, which increases PWV and SBP. This is clear in both figures 6 and 7. However, the relation is also slightly nonlinear: the response is flatter for low SBP than it is for higher SBP. This is clearly visible in the Bland-Altmann analysis, where a linear error trend is visible for each subject (each subject denoted by a distinct color). This stronger increase could be because the legs are actively involved in the physical activity. This causes a stronger increase in PWV to the leg than to other limbs due to local vasoconstriction. This might indicate that when using PWV for the tracking of SBP during physical activity, the relationship between PWV and SBP could be altered in the limb that is involved in the physical activity.

6. Conclusions

While PWV to all sensor locations does show significant correlation with SBP, there are clear advantages and drawbacks associated with each location. The ear PWV as a proximal location has its theoretical advantage of being less affected by vasomotion and orthostatic pressure changes, however a larger inter-subject variability was found in the calibration between SBP and PWV. This should be accounted for in the design of an ear-based PWV measurement system. The wrist location, attractive for the widespread use of PPG in wrist watches, was shown to be equivalent in all tests to the finger PPG. This finding suggests that the many positive results obtained for finger PPG in the past are translatable to a wrist-based measurement system, however also the drawbacks of the finger PPG sensor location might also be inherited, such as the strong effects of orthostatic pressure and vasocontriction. The effect of thermoregulatory vasoconstriction on the wrist remains to be studied. The ankle PPG, being the most distal sensor location, was already expected to perform less well as it can suffer greatly from the many hemodynamic variables over the arterial path. The positive property of the ankle however is that it is easier to accurately estimate PWV since measurement errors in PATs propagate into

smaller PWV estimation errors than they do in more proximal locations. This study suggests that the ankle is indeed too distal for measurement, however these findings should be interpreted with care as a fitness intervention involving the legs was performed.

References

Ankle Brachial Index Collaboration 2008 Ankle-brachial index combined with Framingham Risk Score to predict cardiovascular events and mortality: a meta-analysis *J. Am. Med. Assoc.* **300** 197

Chase J G, Starfinger C, Lam Z, Agogue F and Shaw G M 2004 Quantifying agitation in sedated ICU patients using heart rate and blood pressure *Physiol. Meas.* **25** 1037

Cutler J A, Sorlie P D, Wolz M, Thom T, Fields L E and Roccella E J 2008 Trends in hypertension prevalence, awareness, treatment, and control rates in united states adults between 1988–1994 and 1999–2004 *Hypertension* **52** 818–27

Drinnan M J, Allen J and Murray A 2001 Relation between heart rate and pulse transit time during paced respiration *Physiol. Meas.* **22** 425

ESH/ESC 2013 2013 ESH/ESC guidelines for the management of arterial hypertension: The Task Force for the management of arterial hypertension of the European Society of Hypertension (ESH) and of the European Society of Cardiology (ESC) *Eur. Heart J.* **34** 2159–219

Fonseca P, Aarts R M, Foussier J and Long X 2014 A novel low-complexity post-processing algorithm for precise QRS localization *SpringerPlus* **3** 1

Foo J Y A, Lim C S, Wilson S J, Williams G R, Harris M A and Cooper D M 2007 Pulse transit time ratio as a potential marker for paediatric crural and brachial blood pressure index *J. Hum. Hypertension* **21** 415–7

Gesche H, Grosskurth D, Küchler G and Patzak A 2012 Continuous blood pressure measurement by using the pulse transit time: comparison to a cuff-based method *Eur. J. Appl. Physiol.* **112** 309–15

Greenland P *et al* 2010 2010 ACCF/AHA guideline for assessment of cardiovascular risk in asymptomatic adults *J. Am. College Cardiol.* **56** e50–103

He D D, Winokur E S and Sodini C G 2012 An ear-worn continuous ballistocardiogram (BCG) sensor for cardiovascular monitoring *Proc. Annual Int. Conf. of the IEEE Engineering in Medicine and Biology Society, EMBS* pp 5030–3

Inan O T *et al* 2015 Ballistocardiography and seismocardiography: a review of recent advances *IEEE J. Biomed. Health Inform.* **19** 1414–27

Karamanoglu M, O'rourke M, Avolio A and Kelly R 1993 An analysis of the relationship between central aortic and peripheral upper limb pressure waves in man *Eur. Heart J.* **14** 160–7

Kortekaas M C, Niehof S P, van Velzen M H, Galvin E M, Stolker R J and Huygen F J 2012 Comparison of bilateral pulse arrival time before and after induced vasodilation by axillary block *Physiol. Meas.* **33** 1993

Li Q and Clifford G D 2012 Dynamic time warping and machine learning for signal quality assessment of pulsatile signals *Physiol. Meas.* **33** 1491

McCombie D B 2008 Development of a wearable blood pressure monitor using adaptive calibration of peripheral pulse transit time measurements *PhD Thesis* Massachusetts Institute of Technology

Mukkamala R, Hahn J-O, Inan O T, Mestha L K, Kim C-S and Hakan T 2015 Toward ubiquitous blood pressure monitoring via pulse transit time : theory and practice *IEEE Trans. Biomed. Eng.* **62** 1879–901

Naschitz J E *et al* 2004 Pulse transit time by R-wave-gated infrared photoplethysmography: review of the literature and personal experience *J. Clin. Monit. Comput.* **18** 333–42

Nitzan M, Khanokh B and Slovik Y 2002 The difference in pulse transit time to the toe and finger measured by photoplethysmography *Physiol. Meas.* **23** 85–93

Padilla J M, Berjano E J, Sáiz J, Rodriguez R and Fácila L 2009 Pulse wave velocity and digital volume pulse as indirect estimators of blood pressure: pilot study on healthy volunteers *Cardiovascular Eng.* **9** 104–12

Payne R A, Symeonides C N, Webb D J and Maxwell S R J 2006 Pulse transit time measured from the ECG: an unreliable marker of beat-to-beat blood pressure *J. Appl. Physiol.* **100** 136–41

Peter L, Noury N and Cerny M 2014 A review of methods for non-invasive and continuous blood pressure monitoring: Pulse transit time method is promising? *Irbm* **35** 271–82

Pickering T G, Hall J E, Appel L J, Falkner B E, Graves J, Hill M N, Jones D W, Kurtz T, Sheps S G and Roccella E J 2005 Recommendations for blood pressure measurement in humans and experimental animals: I. Blood pressure measurement in humans: a statement for professionals from the subcommittee of professional and public education of the American Heart Association Council on high blood pressure research *Hypertension* **45** 142–61

Poon C, Zhang Y-T and Liu Y L Y 2006 Modeling of pulse transit time under the effects of hydrostatic pressure for cuffless blood pressure measurements *2006 3rd IEEE/EMBS International Summer School on Medical Devices and Biosensors* pp 65–8

Proença J, Muehlsteff J, Aubert X and Carvalho P 2010 Is pulse transit time a good indicator of blood pressure changes during short physical exercise in a young population? *2010 Annual Int. Conf. of the IEEE Engineering in Medicine and Biology Society (EMBC)* (Piscataway, NJ: IEEE) pp 598–601

Rapalis A, Janusauskas A, Lukosevicius A and Marozas V 2014 Noise resistant method for cardiac pulse wave arrival time estimation *Elektronika ir Elektrotechnika* **20** 59–62

Rupp T L and Balkin T J 2011 Comparison of motionlogger watch and actiwatch actigraphs to polysomnography for sleep/wake estimation in healthy young adults *Behav. Res. Methods* **43** 1152–60

Smith R P, Argod J, Pépin J-L and Lévy P A 1999 Pulse transit time: an appraisal of potential clinical applications *Thorax* **54** 452–7

Solà J, Vetter R, Renevey P, Chételat O, Sartori C and Rimoldi S F 2009 Parametric estimation of pulse arrival time: a robust approach to pulse wave velocity *Physiol. Meas.* **30** 603

SPRINT Research Group 2015 A randomized trial of intensive versus standard blood-pressure control *N. Engl. J. Med.* **373** 2103–16

Sun S, Bezemer R, Long X, Muehlsteff J and Aarts R M 2016a Systolic blood pressure estimation using PPG and ECG during physical exercise *Physiol. Meas.* **37** 2154

Sun S, Bezemer R, Long X, Muehlsteff J and Aarts R M 2016b Systolic blood pressure estimation using ppg during physical exercise *Proc. Annual Int. Conf. of the IEEE Engineering in Medicine and Biology Society, EMBS* p 2415

Tang Z, Tamura T, Sekine M, Huang A, Chen W, Yoshida M, Sakatani K, Kobayashi H and Kanaya S 2016 A chair-based unobtrusive cuffless blood pressure monitoring system based on pulse arrival time *IEEE J. Biomed. Health Inform.* **99** 1

Teng X-F and Zhang Y-T 2007 Theoretical study on the effect of sensor contact force on pulse transit time *IEEE Trans. Biomed. Eng.* **54** 1490–8

Thomas S S, Nathan V, Zong C, Soundarapandian K, Shi X and Jafari R 2015 BioWatch: a non-invasive wrist-based bloodpressure monitor that incorporates training techniques forposture and subject variability *IEEE J. Biomed. Health Inform.* **20** 1291–3000

U.S. Food and Drug Administration 2015 *General Welness Policy for Low Risk Devices — Draft Guidance for Industry and Food and Drug Administration Staff*

Valenti G and Westerterp K 2013 Optical heart rate monitoring module validation study *2013 IEEE Int. Conf. on Consumer Electronics (ICCE)* (Piscataway, NJ: IEEE) pp 195–6

van Andel J, Ungureanu C, Aarts R M, Leijten F and Arends J 2015 Using photoplethysmography in heart rate monitoring of patients with epilepsy *Epilepsy Behav.* **45** 142–5

Wijshoff R, Mischi M and Aarts R M 2016 Reduction of periodic motion artifacts in photoplethysmography *IEE Trans. Biomed. Eng.*

Winter D A 2009 *Biomechanics and Motor Control of Human Movement* (New York: Wiley)

Wong M Y-M, Poon C C-Y and Zhang Y-T 2009 An evaluation of the cuffless blood pressure estimation based on pulse transit time technique: a half year study on normotensive subjects *Cardiovascular Eng.* **9** 32–8

Yoon G, Lee J Y, Jeon K J, Park K-K, Yeo H S, Hwang H T, Kim H S and Hwang I-D 2002 Multiple diagnosis based on photoplethysmography: hematocrit, spo2, pulse, and respiration *Photonics Asia 2002* (International Society for Optics and Photonics) pp 185–8

Zhang G, Gao M, Xu D, Olivier N B and Mukkamala R 2011 Pulse arrival time is not an adequate surrogate for pulse transit time as a marker of blood pressure *J. Appl. Physiol.* **111** 1681–6